International Journal of Refractory Metals and Hard Materials

Research on the effects of solution acidity on microstructure, mechanical and wear properties of tungsten alloys reinforced by yttria - stabilized zirconia particles

--Manuscript Draft--

Manuscript Number:	
Article Type:	Research Paper
Keywords:	Tungsten alloy; Doped zirconia; Yttria - stabilized zirconia; Compressive strength
Corresponding Author:	Fangnao Xiao Univ. Bourgogne Franche-Comte, FEMTO-ST INSTITUTE, CNRS/UFC/ENSMM/UTBM, Department of Applied Mechanics FRANCE
First Author:	Fangnao Xiao
Order of Authors:	Fangnao Xiao
	Thierry Barriere
	Gang Cheng
	Qiang Miao
	Shizhong Wei
	Liujie Xu
Abstract:	Yttria - stabilized zirconia particles (Zr(Y)O 2) strengthened tungsten alloys (W-Zr(Y)O 2) were developed via azeotropic distillation method combined with powder metallurgy techniques. The effects of acidity and alkalinity of the original solution on the precursor powders' morphology, microstructure and the mechanical and wear properties of alloys were deeply investigated. The results showed that the precursor' powder synthesized under solution with pH of 2 possesses finer particles' size. The grain sizes of W-Zr(Y)O 2 alloys prepared with the solutions of different pH values are in the range of 2 - 6 μm, much smaller than that of pure tungsten. When pH value increases from 2 to 8, more and more bonding Zr(Y)O 2 particles are observed. W-Zr(Y)O 2 alloy prepared with the solution of pH equal to 2 have a better microstructure and compressive properties compared to the other two alloys prepared with the solution of pH values of 5 and 8, respectively. Due to the complicated abrasion mechanism, the wear resistance of W-Zr(Y)O 2 alloy increases firstly and then decreases with increase in the doping amount of Zr(Y)O 2 . It is confirmed that the pH 2 value and chemical composition of the tungsten with alloy 3.0 wt. % Zr(Y)O 2 exhibits the highest wear resistance. The abrasion mechanism was analysed in details.

June 21, 2020

To Prof Z.Z. Fang

Editor-in-Chief: Int. J. Refract. Met. Hard Mater.

I am pleased to submit our research article entitled “Research on the effects of solution acidity on microstructure, mechanical and wear properties of tungsten alloys reinforced by yttria stabilized zirconia particles” for publication in Int. J. Refract. Met. Hard Mater.

With the development of accurate, efficient and innovative powder metallurgy process, demand for high - quality powders is also increasing. To improve the quality of tungsten powders for preparing high - performance tungsten products, over the past several years, the liquid - liquid doping techniques, were introduced to synthesize doped tungsten powders. Compared to conventional solid - solid or solid - liquid doping methods, using liquid - liquid doping techniques can avoid the introduction of detrimental contaminants and doping phase evenly distributed in tungsten powders and alloys. However, the prepared doped tungsten powders also exhibit high degree of agglomeration.

The physical and chemical characteristics of the precursor powder, calcination process and reduction process greatly affected the resultant reduced powders. However, the previous researches mainly investigated the effect of liquid - liquid on the mechanical properties of the alloys. Little research concerned on the relationship between precursor powders and microstructure of alloys obtained by liquid - liquid methods. As different polytungstate species exist in aqueous solutions of different acidities, which have a great effect on the morphology and distribution of oxide particles in precursor and reduced powders, we proposed and focused on investigating the effect of acidity solution on precursor powders, microstructure and mechanical and wear properties of W-Zr(Y)O_2 alloy.

In this research, the precursor powders and alloys obtained with different pH values of 2, 5 and 8, were prepared and compared. We found that solutions with different pH values have a litter effect on the tungsten grain size. However, alloy prepared under

solution with pH of 2 processes finer precursor and $Zr(Y)O_2$ particle size, higher relative density, compressive strength compared to alloys prepared under pH value of 5 and 8. Moreover, the wear resistance conducted on alloy prepared under pH value of 2 was investigated in details.

Now, we would submit the manuscript, which is in correct order upon submission according to the guide for authors. With the submission of this manuscript, I would like to undertake that it has not been published elsewhere, has not been accepted for publication elsewhere, and is not under editorial review for publication elsewhere, and that my institute representative is fully aware of this submission.

Furthermore, before submitting this paper, the content was analysed by the Turnitin software to ensure it is without plagiarism.

We would be grateful if the paper could be reviewed in Int. J. Refract. Met. Hard Mater.

Thank you for your consideration.

Fangnao Xiao

2020/6/21

Highlights

1. A chemical doping process is applied to fabricate W-Zr(Y)O_2 alloys.
2. Effect of solution's acidity on the microstructure of W alloy was investigated.
3. Precursor synthesized under pH of 2 has a fine particle - size about 1 - 5 μm.
4. Grain sizes of W alloys prepared in multiple acidity solution are from 2 - 6 μm.
5. Maximal values of compressive strength and failure strain reach 1009 MPa and 0.22.

Graphical Abstract

Present research focus on the influence of various acidity solutions on ODS-W material properties.

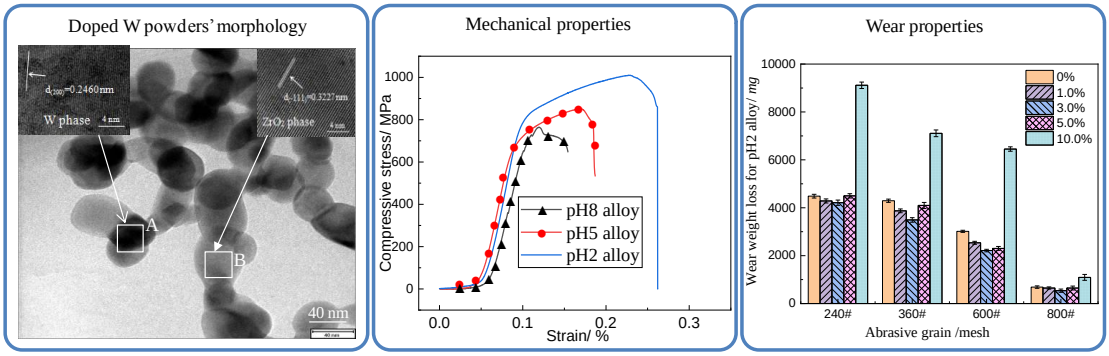

Research on the effects of solution acidity on microstructure, mechanical and wear properties of tungsten alloys reinforced by yttria - stabilized zirconia particles

Fangnao Xiao [a, b, c], Thierry Barriere [a], Gang Cheng [b], Qiang Miao [c], Shizhong Wei [d], Liujie Xu[d]

[a] Univ. Bourgogne Franche-Comté, FEMTO-ST Institute, CNRS/UFC/ENSMM/UTBM, Department of Applied Mechanics, 25000 Besançon, France

[b] INSA CVL, Univ. Tours, Univ. Orléans, LaMé, 3 rue de la Chocolaterie, BP 3410, 41034 Blois Cedex, France

[c] College of Material Science and Technology, Nanjing University of Aeronautics and Astronautics, 29 Yudao Street, Nanjing 210000, China

[d] National Joint Engineering Research Center for abrasion control and molding of metal materials, Henan University of Science and Technology, Luoyang 471003, China

* Corresponding author

Fangnao Xiao

E-mail: fangnao.xiao@ univ-fcomte.fr

Full postal address:

FEMTO-ST Institute, Departement of Applied Mechanics, 24 chemin de l'épitaphe, 25000, Besançon, France

Tel.: +33381666000

Abstract: Yttria - stabilized zirconia particles ($Zr(Y)O_2$) strengthened tungsten alloys (W-$Zr(Y)O_2$) were developed via azeotropic distillation method combined with powder metallurgy techniques. The effects of acidity and alkalinity of the original solution on the precursor powders' morphology, microstructure and mechanical and wear properties of alloys were deeply investigated. The results showed that the precursor' powder synthesized under solution with pH of 2 possesses finer particles' size. The grain sizes of W-$Zr(Y)O_2$ alloys prepared with the solutions of different pH values are in the range of 2 - 6 μm, much smaller than that of pure tungsten. When pH value increases from 2 to 8, more and more bonding $Zr(Y)O_2$ particles are observed. W-$Zr(Y)O_2$ alloy prepared with the solution of pH equal to 2 have a better microstructure and compressive properties compared to the other two alloys prepared with the solution of pH values of 5 and 8, respectively. Due to the complicated abrasion mechanism, the wear resistance of W-$Zr(Y)O_2$ alloy increases firstly and then decreases with increase in the doping amount of $Zr(Y)O_2$. It is confirmed that the pH 2 value and chemical composition of the tungsten alloy with 3.0 wt. % $Zr(Y)O_2$ exhibits the highest wear resistance. The abrasion mechanism was analysed in details.

Keywords: Tungsten alloy; Doped zirconia; Yttria - stabilized zirconia; Compressive strength.

Nomenclature

BSE	Backscattered electron
DSC	Differential scanning calorimeter
EDS	Electron dispersive spectroscopy
HV	Vickers hardness
HR - TEM	High - resolution transmission electron microscopy
L - L	Liquid - liquid
ODS - W	Oxide particles dispersion - strengthened tungsten

SAEDP	Selected area electron diffraction pattern
SEM	Scanning electron microscope
TGA	Thermogravimetric analysis
XRD	X - ray diffraction

1. Introduction

Tungsten alloys have been widely used in the defence industry, nuclear reactor, and space vehicle equipment, thanks to its high melting point, high hardness, high strength at room and high temperature [1 - 4]. Especially, the researches on the oxide dispersion - strengthened tungsten (ODS - W) have attracted considerable attentions [5 - 6], as these stable oxide particles could decrease the ductile - brittle transition temperature and increase the recrystallization temperature [7, 8].

The past several years, many of liquid - liquid (L - L) methods were introduced to prepare the ODS - W alloys [9 - 13]. However, the previous researches mainly focus on the mechanical properties of the alloys, such as bending, tensile, and torsional fatigue strengths [14]. Little research concerned the relationship between precursor powders and microstructures of alloys obtained by L - L methods. Actually, as previous researches in this area have been reported [2, 9, 12, 14], the morphology and composition of the precursor greatly affected the morphology and distribution of oxide particles in reduced powders, which further affected the tungsten grain size, eventual oxide particles' size and their distribution. It was reported [15] that the solutions with different acidities had a great effect on the reduced tungsten powders. The researches concerning the effect of the solution acidity and alkalinity on precursor powders, microstructure and mechanical and wear properties of tungsten alloys have to be investigated in detail.

In this research, the precursor powders and alloys obtained with different pH values of 2, 5 and 8 (the corresponding powders / alloys were denoted as pH 2, pH 5 and pH 8 powders / alloys below), were prepared and investigated. The morphologies of precursor powders were analysed. Proper calcination process was determined through thermogravimetric analysis and differential scanning calorimetry. The

microstructure, mechanical properties and abrasion resistance of alloys were compared to study the effect of acidity and alkalinity of the solution.

This paper is structured as follows. In Section 2, the preparation process and methods of measurement and analysis of pure and doped tungsten alloy are introduced in detail. In Section 3, the morphology of precursor powders, the calcination process and the reduced powders are investigated, respectively. The microstructures of W-Zr(Y)O_2 alloys prepared under different pH values are investigated and compared. In Section 4, the relative density, compressive strength and abrasion resistance of alloys prepared under different pH values are described. The main results are presented in Section 5, and concludes with a brief discussion the paper.

2. Experimental procedure

2.1 Chemical composition and preparation of alloys

In this research, two kinds of tungsten alloy samples with different compositions, shown in Table 1, were elaborated via the azeotropic distillation method combined with the powder metallurgy method. The commercial $Zr(NO_3)_4{\cdot}5H_2O$, $Y(NO_3)_3{\cdot}6H_2O$ and ammonium metatungstate $(NH_4)_6H_2W_{12}O_{40}{\cdot}xH_2O$ were retained as raw materials. All materials of high - purity (99.9%) have been selected. Firstly, these raw materials were dissolved in distilled water, respectively. Then, the $Zr(NO_3)_4{\cdot}5H_2O$ and $Y(NO_3)_3{\cdot}6H_2O$ solutions were mixed together. The $(NH_4)_6H_2W_{12}O_{40}{\cdot}xH_2O$ solution, was added drop by drop, to previous mixed solution to elaborate the original solution. Finally, the pH value of the original solution was adjusted using nitric acid or ammonia solution and fiercely stirring at a room temperature for 5 h. The distillation process of azeotropic method was reported elsewhere [15]. The synthesized precursor powders were calcined and reduced by following two reduction processes 750 ℃ × 2 h + 900 ℃ × 4 h under hydrogen atmosphere in order to achieve W-Zr(Y)O_2 powders.

The W-Zr(Y)O_2 powders were pressed into a rubber mould at 350 MPa pressure for 30 minutes using cold isostatic press to obtain cylindrical billets that is 30 mm long with a diameter of 20 mm. The samples were then placed into a medium - frequency induction sintering furnace under hydrogen atmosphere. The pre - sintering

temperature was performed of 1250 °C (2 h). The final sintering temperature was set at 2400 °C for 4 h. Finally, the W-Zr(Y)O_2 alloys were obtained.

Table 1. The chemical composition of the tungsten alloy samples (wt. %).

Samples	**W**	**ZrO_2**	**Y_2O_3**
Pure W	100	0	0
Doped W	96.62	3.0	0.38

2.2 Measurement and analysis

The absolute densities of the tungsten alloys were evaluated using Archimedes principle. The relative densities were calculated based on the method reported in [12].

Vickers hardness measurement was tested using a micro - Vickers hardness tester (HVS - 1000 A) with a load of 200 g and a dwell time of 20 s. The Vickers hardness value of each sample was an average of 10 readings taken at random sample locations. Compression tests were carried out at room temperature using a universal material testing machine (AG - I250 KN) at a crosshead speed of 1.0 mm / min.

The wear properties of the alloys were studied using a pin - on - dish (ML - 100 type) wear test apparatus testing machine with different grit alumina waterproof - abrasive sandpapers of 240, 360, 600 and 800, respectively, under constant load of 40 N. The dimensions of the cylindrical samples are: diameter 6 mm × length 20 mm. Each sample moved repeatedly for 20 times. Before and after wear tests, the samples were washed with ethanol and were weighted using a digital micrometer with a least count of 0.1 mg. For each tungsten alloy, at least three samples were selected, and the wear weight loss for each sample was an average value of the three repetitions.

The morphology, microstructure and chemical composition of powders and alloys' samples were observed via scanning electron microscope (SEM), backscattered electrons (BSE) and an energy - dispersive X - ray spectrometry (EDS), respectively. The reaction processes of precursor powders were analysed by thermogravimetric analysis (TGA) and differential scanning calorimeter (DSC) using

a NETZSCH STA 409 PC/PG thermal analyser. High - resolution transmission electron microscopy (HR - TEM) was employed to observe the microstructure.

3 Results and discussions

3.1 Analysis of precursor powders synthesized under different pH values

Fig. 1 a), b) and c) shows the SEM images of precursors synthesized through azeotropic distillation method corresponding to three different pH values of 2, 5 and 8. In Fig. 1 a) corresponding to case study for pH 2 investigated by F. Xiao and al. [9], the particles possess granular structure with a size of approximately 1 - 5 μm, while a small number of particles are plate - like structure. The morphology of the precursor powder is mainly plate-shaped and block-shaped, as shown in Fig. 1 b) (case study for pH 5). The length of the plate-shaped particle is less than 10 μm, the particle surface is smooth and the dispersion is well. The particles mainly show a blocky structure with a particle size of 3 - 8 μm, as shown in Fig. 1 c) (case study for pH 8). The morphology of the precursor powders was affected significantly by the pH value of solution.

The particle size increases and the morphology changes greatly with the pH value of the solution. This is mainly due to the different polytungstate species existed in solutions resulted from different pH values. Previous research by F. Xiao and al. [15] shown in detail, the reaction' mechanism between polytungstate species with H^+/ OH^- were discussed in detail.

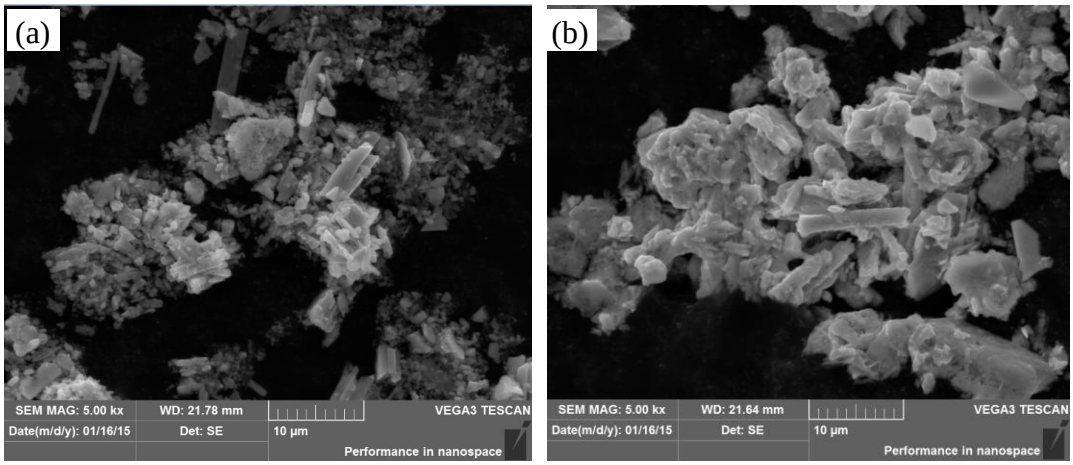

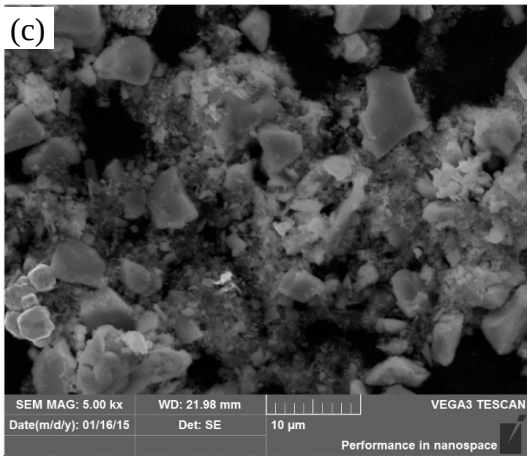

Fig. 1 SEM images of the precursor powders synthesized under different pH values for doped tungsten sample: a) pH 2 [9], b) pH 5 and, c) pH 8.

3.2 Analysis of calcined and reduced powders conducted on doped pH 2 precursor powder

The pH 2 precursor powder particle possesses finer particle structure according to the analysis in section 3.1. The TGA and DSC analyses were carried out to determine the calcination process of pH2 precursor powder, as shown in Fig. 2. When the temperature rises to 140 - 160 ℃, a small range of endothermic peak appears, which is caused by the evaporation of partially adsorbing free water in the precursor powder. At 308.3 ℃, there is an obvious exothermic peak, which is caused by the decomposition of reaction product NH_4NO_3, accompanying by a small amount of mass loss. However, when the temperature increases to about 360 ℃, a sharp endothermic peak appears, this is due to the loss of crystalline water in the reaction products. The exothermic peak occurring at 417.3 ℃ is attributed to the transformation from WO_3 amorphous to WO_3 crystal. When the temperature increases to 550 ℃, the total mass loss of the sample is about 7.9 %. When the temperature continues to increase, the TGA curve in Fig. 2 shows that the mass loss is almost unchanged, which indicates that the precursor powder is almost completely decomposed at 550 ℃.

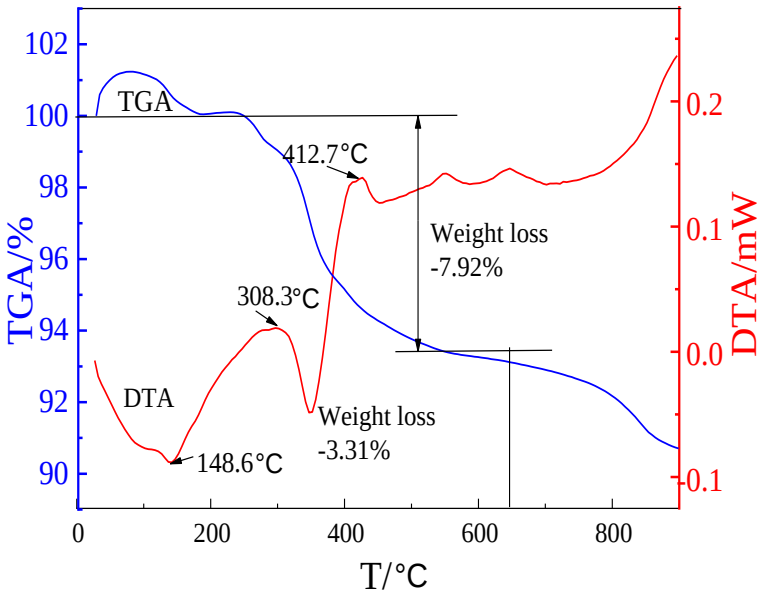

Fig. 2 TGA - DSC curves of doped tungsten precursor powder synthesized under pH 2.

The reduced pH 2 powder was analysed by HR - TEM to determine the particle morphology and phase structure of the reduced powder. The HR - TEM images of the reduced powder reduced after 750 ℃×2 h + 900 ℃ × 4 h are shown in Fig 3 a). Based on Fig. 3 a), the reduced powder presents a small spherical particle shape with regular morphology and well-dispersed. The particle size is about 40 nm, which belongs to nano-sized particles. The selected area A correspond to Fig. 3 b). As the nanoparticle under selected area B consists of the containing - Zr phase and containing - Y phase through mixing these two phases firstly, the selected area B correspond to Figs. 3 c) and, d). The reduced powder particles were calibrated with lattice fringes, as shown in Figs. 3 b), c) and d). The measured spacing of lattice fringes are 0.2460 nm, 0.3227 nm and 0.3448 nm, respectively, which are close to the spacing of W (200), ZrO_2 (-111) and Y_2O_3 (202) crystal planes of PDF#47-1319, PDF#65-2357 and PDF#44-0399, respectively [17]. As analysis above, the reduced pH 2 powder is composed of tungsten and ZrO_2-Y_2O_3 nano-sized particles.

The formation of nano-sized ZrO_2-Y_2O_3 doped tungsten powder is related to the formation mechanism of doped tungsten powder during hydrogen reduction process. During high - temperature reduction, Y and Zr atoms are always in the form of oxide,

solid tungsten oxide would volatilize and then form hydroxide $WO_2(OH)_2$ with high volatility. As the reduction reaction continues, hydroxide $WO_2(OH)_2$ would deposit on the surfaces of the neighbour tungsten oxide with low valence states or doped Y_2O_3-ZrO_2 particles [18]. The increase in growth rate and "volatilization - deposition" would make tungsten particles full growth in the reduction process [19]. The existence of Y_2O_3-ZrO_2 particles provides the plenty of crystal nucleus, which hinders the growth of tungsten particles, eventually forming the nano-sized doped tungsten powder.

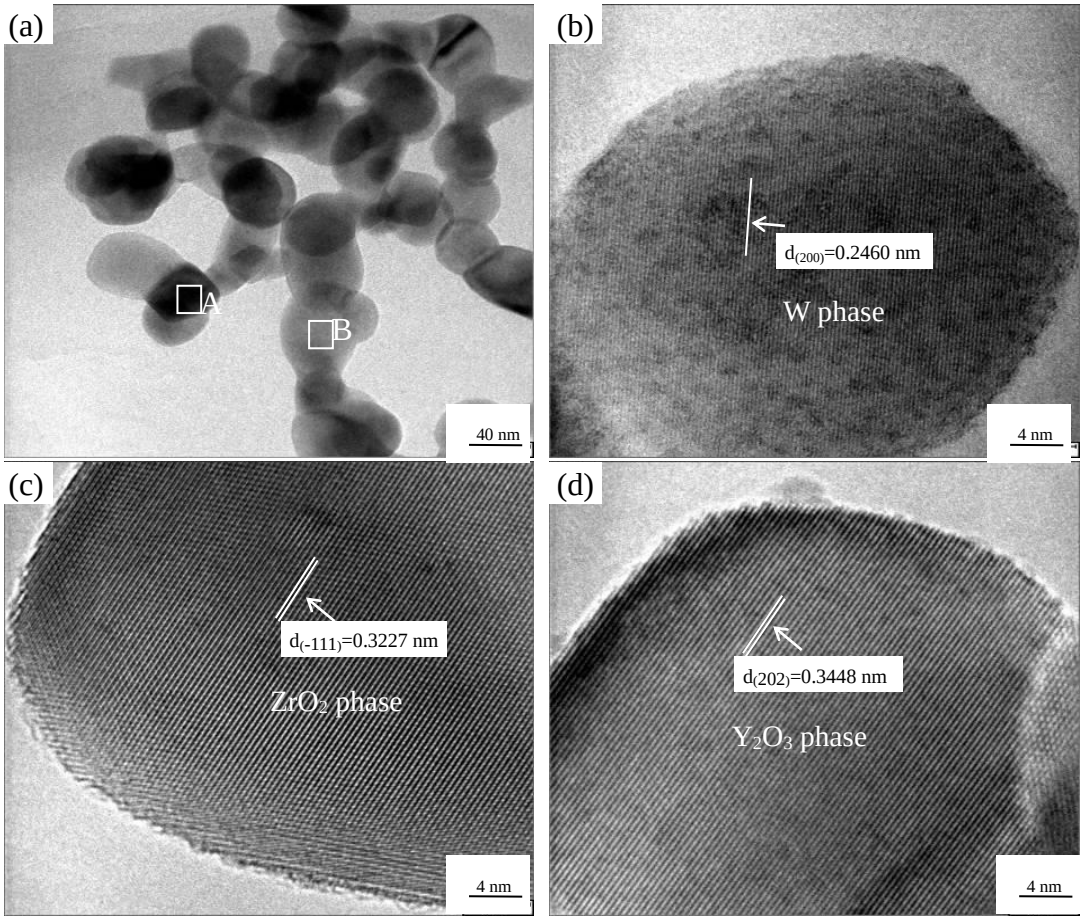

Fig. 3 HR - TEM image and diffraction fringes of reduced powders corresponding to test case pH 2 for doped W sample: a) HR - TEM image of reduced powders, b) Diffraction fringes of W powder particle, c) Diffraction fringes of ZrO_2 powder particle and, (d) Diffraction fringes of Y_2O_3 powder particle.

3.3 Microstructure and phase structure analysis of tungsten alloys

The BSE images of pure W and W-$Zr(Y)O_2$ doped alloys prepared under different pH values are shown in Fig. 4. Based on the EDS analysis, the black phase belongs to $Zr(Y)O_2$ consisting of three elements (Zr, Y, O). Selected - area electron diffraction patterns (SAEDP) indicate that ZrO_2 particles belong to the stabilized ZrO_2 phase as shown in Fig. 5.

Fig 4 a) shows that the grains size of pure tungsten is relative uniform compared to the other alloys. The grain size of the irregular particles is about 10 - 15 μm. Based on Figs. 4 (b - d), it is obvious that there are a large number of pores among alloys which is mainly caused by the pressure less sintering process. Thus, the densities of alloys are much lower than pure tungsten alloy. In these alloys, the grain size is almost same in range of 2 - 6 μm, much smaller than pure tungsten alloys. This is due to the grain refinement effect of the $Zr(Y)O_2$ particles. Based on the BSE images, most of these particles are with the size larger than 2 μm at least and mostly located at W grain boundaries. However, lots of nano-sized $Zr(Y)O_2$ particles among alloy was found according to TEM results in Fig. 5b.

Detailed observation shows the differences in morphology and distribution of $Zr(Y)O_2$ particles are observed among different W-$Zr(Y)O_2$ alloys. When the alloy was prepared under pH value of 2, the $Zr(Y)O_2$ particles was smaller in size and distributed more uniformly compared to the other two alloys. Few bonding particles were observed. However, increasing pH value to 5, the occurrence of some obvious bonding $Zr(Y)O_2$ particles can be found marked by arrow A. When pH value increased to 8, more and more bonding particles were observed, which was not conducive to the improvement of alloy properties.

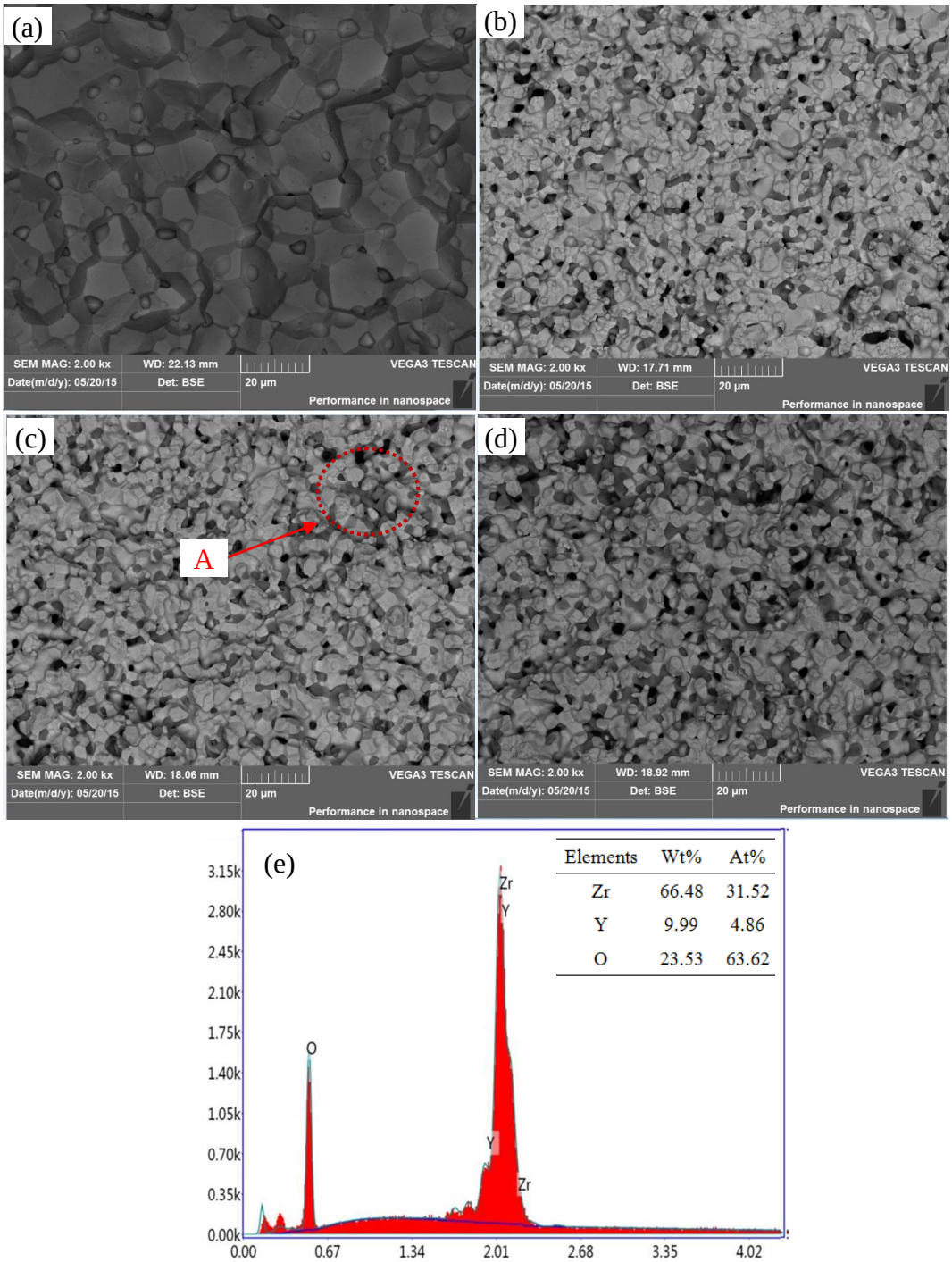

Fig. 4 Microstructure BSE images and of EDS patterns pure and doped tungsten alloys: a) Pure W, b) pH 2, c) pH 5, d) pH 8 and, e) EDS patterns of doping phase.

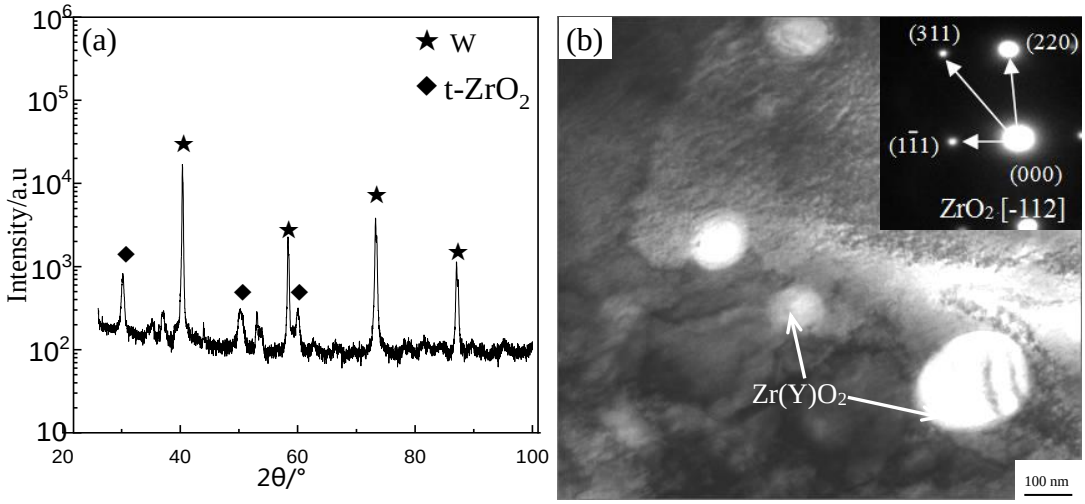

Fig. 5 (a) XRD patterns of test case pH 2 for doped W sample, b) HR - TEM image of test case pH2 for doped tungsten sample [9].

The stabilized ZrO_2 phase among alloy has been elaborated as analysis above. At high temperature, stabilized zirconia with $Zr\text{-}O_8$ structure consists of a zirconium ion and eight equidistant oxygen ions. However, as the temperature decreases, according to Coordination Theory, due to $rZr^{4+}/rO^{2-} = 0.564$ (less than 0.732), eight - coordinate structure in ZrO_2 phase would decrease the interspace between oxygen atoms. It would lead to the increasing of the coulomb repulsion between adjacent oxygen - oxygen ions. As a result, the original crystal structure would become unstable, and then promote the transformation from stabilized structure to monoclinic structure with $Zr\text{-}O_7$ [20].

However, as shown in Fig. 6, Y^{3+} as stabilizer from Y_2O_3 particles could replace the partial Zr^{4+} atoms in ZrO_2 at high temperature, increasing the cation - anion radius ratio. Meanwhile, oxygen vacancies are introduced into the lattice to remain charge neutrality of ZrO_2 phase. It would increase the interspace of oxygen - oxygen and reduce the repulsive forces between the local oxygen - oxygen, and then promote the formation of the stability of the $Zr\text{-}O_8$ structure.

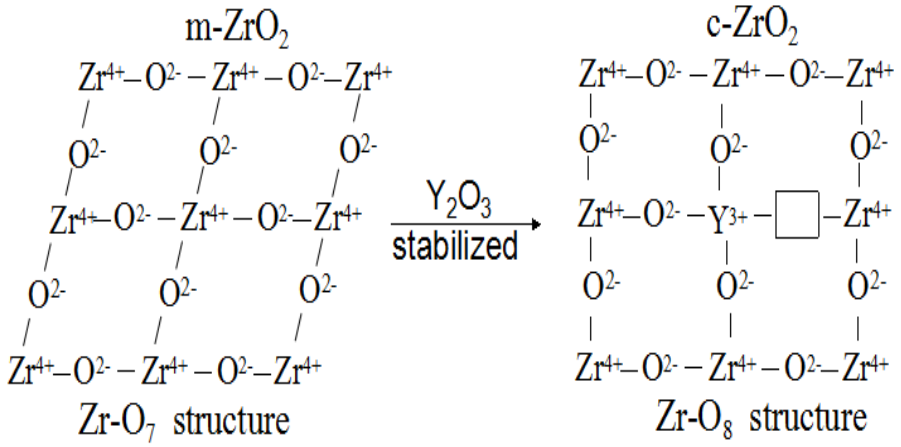

Fig. 6 Schematic flowchart of the cubic yttria - stabilized zirconia.

4. Mechanical properties of W-Zr(Y)O_2 alloy

4.1 Compressive properties of W-Zr(Y)O_2 alloy

The compressive properties of alloys elaborated with different pH values of 2, 5 and 8 were compared in Fig. 7 a). The pH 2 alloy exhibits highest compressive strength and failure strain value compared to pH 5 and pH 8 alloys. The ultimate compressive strength and failure strain value of pH 2 reach to 1009 MPa and 0.22, respectively. The compressive strength and the failure strain value of the alloy increase at lower pH values.

The compressive strength value of pH 2 alloy is approximately 252 MPa much less than pure tungsten, as shown in Fig. 7 b). The enrichment zone of oxide particles caused by the high content of oxide particles results in mutual superposition of stress field distribution around the reinforced particles [15]. It leads to the fact that weakening effect on strength in alloy is greater than the strengthening effect caused by dislocation motion, which weaken the bonding strength of the W - W grain boundaries and the fracture strain of W-Zr(Y)O_2 alloy.

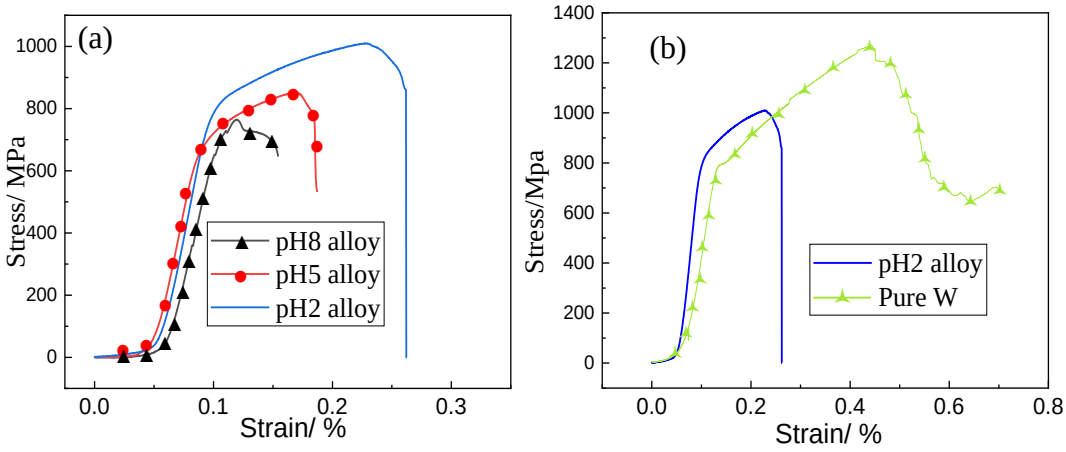

Fig. 7 Compressive stress - strain curves of tungsten alloys: a) Doped tungsten alloys prepared under different pH values and, b) Pure and doped tungsten alloys.

Table 2 shows the relative density, micro-hardness and wear resistance of pure and doped tungsten alloys. The relative density of the pure tungsten is about 97.9%, higher than that of pH2 alloy (i.e. 90.9%). The micro-hardness of the pH2 alloy is lower than that of the pure tungsten. This may be due to the fact that the pores emerging in the sintering process lead to damage the metallic continuity and reduce its effective area.

Table 2 Density, micro-hardness and abrasion loss of pure and doped tungsten alloys.

Alloys	**Relative density (%)**	**Micro-hardness (HV)**	**Abrasion loss (mg)** [a*]
Pure tungsten	97.9±0.3	367 ± 15	4292 ± 100
Doped alloy (pH 2)	90.9±0.5	349 ± 30	3490 ± 100

a* Wear resistance test was carried out using 360 grit Al_2O_3 waterproof - abrasive sand paper under the loading of 1.40 N/mm^2.

4.2 Effect of Zr(Y)O_2 on wear resistance of tungsten alloy

Based on the above analysis, the pH 2 alloy exhibits better mechanical properties. Therefore, the effect of zirconia on wear resistance of pH 2 alloy was investigated.

Figs. 8 a) and b) show the influence of abrasive particle size and applied load on the wear resistance properties of W-Zr(Y)O_2 alloys.

Based on Fig. 8 a), the weight loss of the alloys decreases with the abrasive particle size ranging from 240 to 800 using the same loading of 1.40 N/mm^2. However, the weight loss of W-Zr(Y)O_2 alloys decreases with the ZrO_2 fraction from 0 to 3 wt.% with the same abrasive particles size (360 grit Al_2O_3 waterproof - abrasive). Then the weight loss of W-Zr(Y)O_2 alloys increases with the ZrO_2 fraction from 3% to 10%. The same observations have been obtained by F. N. Xiao and al. with similar results [12] shown in Fig 8 b), which indicates that W-3.0%Zr(Y)O_2 alloy has the best wear resistance properties.

Because the hardness of Zr(Y)O_2 particles is higher than that of the tungsten matrix, during abrasive wear testing, the abrasive particles mainly interact with the Zr(Y)O_2 particles. The tungsten matrix is in the lower wear zone, which reduces the wear loss of tungsten matrix. Moreover, more internal pores in alloys are obtained with the increase of Zr(Y)O_2 content, which decreases the bonding strength between Zr(Y)O_2 and tungsten matrix. In the wear process, the abrasive particles firstly contact with the Zr(Y)O_2 particles and the higher load results in the Zr(Y)O_2 particles falling off from the tungsten matrix. As a result, the Zr(Y)O_2 particles and the abrasive particles (Al_2O_3) aggravate the wear loss rate of alloy together [21].

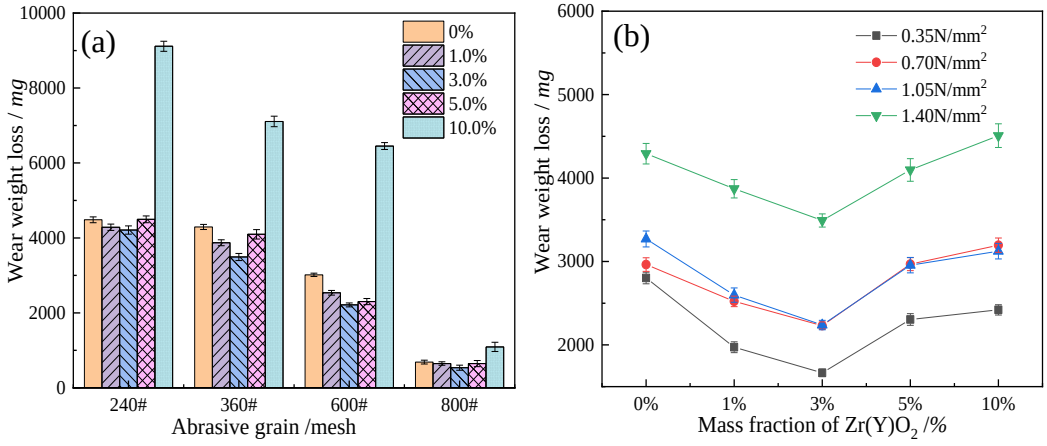

Fig. 8 Effect of abrasive particle size and applied load on the wear weight loss of W-Zr(Y)O_2 alloys under different conditions: a) Abrasive particle size measured at 1.40 N/mm^2, b) Applied load for abrasive grain size of 360 [12].

5. Conclusion

1. Different precursor powders were synthesized under different pH values of 2, 5 and 8, respectively. Morphologies of these precursor powders were compared, as well as the microstructures, mechanical and wear properties of their corresponding alloys,

2. The precursor' powder synthesized under solution with pH value of 2 possesses finer particles' structure. The effects of calcination process was investigated to optimize the calcination procedure through thermogravimetric analysis and differential scanning calorimeter,

3. W-Zr(Y)O_2 alloy, prepared under pH value of 2, has a better microstructure and compressive properties over other two alloy studied in this investigation (i.e. pH values equal 5 and 8), respectively,

4. The effects of Zr(Y)O_2 mass fraction on the abrasive wear resistance of tungsten alloy under different conditions were investigated. The abrasion mechanism was analysed in details. Various mechanical properties of W-Zr(Y)O_2 alloy prepared under pH of 2, such as relative density, compressive strength and abrasion resistance, were compared to pure tungsten.

Declaration of interest

There are no conflicts to declare.

Founding: This work is supported by National Natural Science Foundation of China [No. 51672070], Henan province science and technology innovation talent plan, China [No. 2017JQ0012] and Graduate Research and Innovation Projects in Jiangsu Province [No. KYCX19_0182].

Acknowledgements

We would like to thank all the researchers who participated in our works discussed in the paper and whose names appear in references.

References

[1] M. Kawai, M. Furusaka, K. Kikuchi, H. Kurishita, R.Watanabe, J. F. Li, K. Sugimoto, T. Yamamura, Y. Hiraoka, K. Abe, A. Hasegawa, M. Yoshiie, H. Takenaka, K. Mishima, Y. Kiyanagi, T. Tanabe, N. Yoshida, T. Igarashi, R&D of a MW-class solid-target for a spallation neutron source, J. Nucl. Mater. 318 (2003) 38-55.

[2] L. J. Xu, F. N. Xiao, S. Z. Wei, Y. C. Zhou, K. M. Pan, X. Q. Li, J. W Li, W. L, Development of tungsten heavy alloy reinforced by cubic zirconia through liquid-liquid doping and mechanical alloying methods, Int. J. Refract. Met. Hard Mater. 78 (2019) 1-8.

[3] A. Upadhyaya, Processing strategy for consolidating tungsten heavy alloys for ordnance applications, Mater. Chem. Phys. 67 (2001) 101-110.

[4] H. Bolt, V. Barabash, W. Krauss, J. Linke, R. Neu, S. Suzuki, N. Yoshida, A. U. Team, Materials for the plasma-facing components of fusion reactors, J. Nucl. Mater. 329 (2004) 66-73.

[5] C. L. Chen, C. L. Huang, Milling media and alloying effects on synthesis and characteristics of mechanically alloyed ODS heavy tungsten alloys, J Alloy Compd. 44(2014) 19-26.

[6] L. Veleva, R. Schaeublin, M. Battabyal, T. Plociski, N. Baluc, Investigation of microstructure and mechanical properties of W-Y and W-Y_2O_3 materials fabricated by powder metallurgy method, Int. J. Refract. Met. Hard Mater. 50 (2015) 210-6.

[7] P. K. Senapati, B. K. Mishra, A. Parida, Modeling of viscosity for power plant ash slurry at higher concentrations: effect of solids volume fraction, particle size and hydrodynamic interactions, Powder Technol. 197, 2010, 1–8. https://doi.org/10.1016/j.powtec.2009.07.005

[8] M. A. Yar, S. Wahlberg, H. Bergqvist, Chemically produced nanostructured ODS-lanthanum oxide-tungsten composites sintered by spark plasma, J. Nucl. Mater, 408 (2011) 129-135.

[9] F. Xiao, L. Xu, Y. Zhou, K. Pan, J. Li, W. Liu, S. Wei, A hybrid microstructure design strategy achieving W-ZrO_2(Y) alloy with high compressive strength and critical failure strain, J Alloy Compd. 708 (2017) 202-212.

[10] Y. T. Cui, J. S. Wang, W. Lui, X. Wang, Effect of scandia on tungsten oxide powder reduction process, J. Rare. Earth. 28 (2010) 202-205.

[11] S. H. Hong, B. K. Kim, Fabrication of W-20 wt% Cu composite nanopowder and sintered alloy with high thermal conductivity, Mater. Lett. 57 (2003) 2761-2767.

[12] F. N. Xiao, L. J. Xu, Y. C. Zhou, K. M. Pan, J. W. Li, W. Liu, S. Z. Wei, Preparation, microstructure, and properties of tungsten alloys reinforced by ZrO_2 particles, Int. J. Refract. Met. Hard Mater. 64 (2017) 40-46.

[13] Y. Han, J. Fan, T. Liu, The effect of trace nickel additive and ball milling treatment on the near-full densification behavior of ultrafine tungsten powder, Int. J. Refract. Met. Hard Mater. 34 (2012) 18-26.

[14] F. N. Xiao, Q. Miao, S. Z. Wei, T. Barriere, G. Cheng, S. W. Zuo, L. J. Xu, Uniform nanosized oxide particles dispersion strengthened tungsten alloy fabricated involving hydrothermal method and hot isostatic pressing, J Alloys Compd, 824 (2020): 153894..

[15] F. N. Xiao, Q. Miao, S. Z. Wei, Z. Li, T. L. Sun, L. J. Xu, Microstructure and mechanical properties of W-ZrO_2 alloys by different preparation techniques, J Alloys Compd, 774 (2019): 210-221.

[16] L. J. Xu, S. Z Wei, Q. Liu, G. S Zhang, J. W. Li, Microstructure and High-Temperature Frictional Wear Property of Mo-Based Composites Reinforced by Aluminum and Lanthanum Oxides, Tribology Transactions, 56 (2013): 833-840.

[17] F. N. Xiao, L. J. Xu, Y. C. Zhou, K. M. Pan, S. Z. Wei, Preparation process and properties of yttria stabilized cubic zirconia reinforced tungsten based alloys, Transactions of Materials and Heat Treatment, 2016, 37(2): 12-19.

[18] F. N. Xiao, Q. Miao, S. Z. Wei, Hydrothermal synthesis of nanoplates assembled hierarchical h-WO_3 microspheres and phase evolution in preparing cubic Zr (Y) O_2-doped tungsten powders, Adv. Powder Technol. 29 (2018) 2633-2643.

[19] P. Lu, C. Y. Shen, T. Qiu. Preparation of sub-micron tungsten powder doped with CeO2[J]. Powder Metallurgy Industry, 2008, 18(2): 6-8.

[20] X. Y.Lu, K. M. Liang, S. R Gu, et al. Influence of oxygen vacancy on phase structure and transformation of zirconia, Journal of the Chinese Ceramic Society, 1996, 24(6): 670-673.

[21] S. Z. Wei, L. J. Xu, Review on Research Progress of Steel and Iron Wear-Resistant Materials. Acta Metall Sin, 2020, 56(4): 523-538.

Declaration of interests

The authors declare that they have no known competing financial interests or personal relationships that could have appeared to influence the work reported in this paper.